

NANO EXPRESS

Open Access



# MoS<sub>2</sub> with Controlled Thickness for Electrocatalytic Hydrogen Evolution

Xiaoxuan Xu<sup>1</sup> and Lei Liu<sup>2\*</sup>

## Abstract

Molybdenum disulfide (MoS<sub>2</sub>) has moderate hydrogen adsorption free energy, making it an excellent alternative to replace noble metals as hydrogen evolution reaction (HER) catalysts. The thickness of MoS<sub>2</sub> can affect its energy band structure and interface engineering, which are the avenue way to adjust HER performance. In this work, MoS<sub>2</sub> films with different thicknesses were directly grown on the glassy carbon (GC) substrate by atomic layer deposition (ALD). The thickness of the MoS<sub>2</sub> films can be precisely controlled by regulating the number of ALD cycles. The prepared MoS<sub>2</sub>/GC was directly used as the HER catalyst without a binder. The experimental results show that MoS<sub>2</sub> with 200-ALD cycles (the thickness of 14.9 nm) has the best HER performance. Excessive thickness of MoS<sub>2</sub> films not only lead to the aggregation of dense MoS<sub>2</sub> nanosheets, resulting in reduction of active sites, but also lead to the increase of electrical resistance, reducing the electron transfer rate. MoS<sub>2</sub> grown layer by layer on the substrate by ALD technology also significantly improves the bonding force between MoS<sub>2</sub> and the substrate, showing excellent HER stability.

**Keywords:** MoS<sub>2</sub>, Atomic layer deposition, Hydrogen evolution, MoS<sub>2</sub> thickness

## Introduction

Hydrogen energy has become an excellent choice for solving global energy shortages and environmental pollution due to its own advantages (such as abundant sources, high energy density, and only water as combustion products) [1–3]. Hydrogen production by electrolysis of water is considered to be a green hydrogen production technology because it can get rid of the dependence on carbon-containing fossil fuels [4, 5]. Although the hydrogen evolution reaction (HER) can produce hydrogen, its high energy consumption and low yield have always been a concern [6]. Platinum (Pt)-based noble metal catalysts have shown strong catalytic activity, but their higher prices and lower reserves have prevented them from being applied in industry [7]. Therefore, exploring and developing non-noble metal catalysts with abundant reserves, low price, high efficiency and durability is an important strategy to promote the application

of hydrogen energy, which has become one of the most important research hotspots [8–10].

At present, transition metal oxides, sulfides, phosphides, nitrides, carbides, alloys and other catalysts have been developed for HER [11–15]. Among them, molybdenum disulfide (MoS<sub>2</sub>) has an activity close to that of Pt in catalytic sites and it becomes a preferred Pt substitute material in non-noble metal chalcogenides theoretically [16]. Unlike the bulk phase, the two-dimensional (2-D) MoS<sub>2</sub> with layered structure exhibits unique surface effects, small size effects, and macroscopic quantum tunneling effects, which greatly improves related HER performance [17, 18]. However, the 2-D MoS<sub>2</sub> is prone to stacking, which reduces the number of edge active sites and affects hydrogen production [19]. In order to make full use of the active sites of MoS<sub>2</sub>, a few layers of MoS<sub>2</sub> are attempted to manufacture. The commonly preparation methods mainly include the “top-down” method represented by the micromechanical force stripping, the lithium ion intercalation, the liquid phase ultrasonic method, and the “bottom-up” method represented by the high temperature thermal decomposition, vapor

\*Correspondence: liulei@seu.edu.cn

<sup>2</sup> School of Mechanical Engineering, Southeast University, Nanjing 211189, People's Republic of China

Full list of author information is available at the end of the article

deposition, hydrothermal method [20–22]. Among them, “top-down” is difficult to achieve high-efficiency reproducible manufacturing and the “bottom-up” is relatively controllable and has a wide range of applications. Chemical vapor deposition (CVD) is a representative method in manufacturing fewer layers of MoS<sub>2</sub> films [23]. Although the MoS<sub>2</sub> films prepared by CVD exhibit high quality, such as a flat surface, less lattice distortion and other defects, CVD cannot uniformly produce MoS<sub>2</sub> on the surface of a structure with a high aspect ratio [24]. In addition, because of low stability and low repeatability, the CVD method cannot be used to manufacture MoS<sub>2</sub> with a large scale.

As a specially modified CVD method, atomic layer deposition (ALD) is also used to fabricate thin film materials [25]. In an ALD cycle, through a self-limiting chemical reaction, a complete reaction is interrupted into two half-reactions [26]. Only when the active sites of surface are exhausted, the first half reaction stops, and then another half reaction will proceed [27]. The chemical reaction of the newly fabricated atomic film is directly determined by the previous layer, so only one layer of atoms can be deposited per ALD cycle [28]. During the ALD process, not only the thickness of the film can be precisely controlled, but the uniformity of the film on the substrate with complex morphology can also be well maintained [29]. In addition, because the manufacturing process is not sensitive to the amount of precursor, ALD has high repeatability. Therefore, ALD is suitable for the controlled manufacture 2-D MoS<sub>2</sub> films [30].

In this work, MoS<sub>2</sub> with different thicknesses were controllably grown on glassy carbon (GC) substrates through ALD technology, and it was directly used as a catalyst for HER without binders. The hydrogen evolution performance of MoS<sub>2</sub>/GC in acid solution was studied, and the related mechanism was also analysed.

## Methods

The current study was aimed to improve the HER performance of MoS<sub>2</sub> by adjusting its thickness.

## Materials

Glassy carbon (GC, 15 mm × 10 mm × 1 mm) was purchased from Beijing Anatech Co., Ltd. Molybdenum pentachloride (MoCl<sub>5</sub>, 99.6%) was purchased from Shanghai Aladdin Bio-Chem Technology Co., Ltd. Hydrogen sulfide (H<sub>2</sub>S, 99.6%) and Nitrogen (N<sub>2</sub>, 99.999%) were received from Nanjing Special Gas Factory Co., Ltd.

## Preparation of MoS<sub>2</sub> on GC

GC with excellent conductivity was used as the substrate for manufacturing the few layers MoS<sub>2</sub> film. The GC was ultrasonically cleaned with acetone, ethanol and

deionized water for 5 min, and then treated with plasma for 5 min. The MoS<sub>2</sub> film was deposited on GC using a commercial ALD equipment (Sunaletmr-100, Picosun). Before depositing process, the reaction chamber and Mo source were heated to 460 °C and 210 °C, respectively, and stabilize for one hour. Then, MoCl<sub>5</sub> and H<sub>2</sub>S were alternately injected into the reaction chamber. The carrier gas used was N<sub>2</sub> and the flow rate was 50 sccm. The pulse time for source and cleaning was 0.5 s, 30 s, 0.5 s and 30 s, respectively. By controlling the number of ALD cycles to 50, 100, 150, 200 and 250, the preparation of MoS<sub>2</sub> films with different thicknesses were achieved.

## Characterization

Scanning electron microscope (SEM) was used to observe the morphology of the catalyst by Inspect-F50 (FEI) instrument, and the acceleration voltage was 20 kV. High resolution-transmission electron microscope (HR-TEM) images were obtained on JEM-2100 (Olympus) instrument, and the acceleration voltage was 200 kV. X-ray diffraction (XRD) was employed to study the crystal phase structure by Smartlab-3 (Rigaku). Raman spectrometer (Raman) was used for analysis of solid surface composition by XperRam C (Nanobase) instrument, and the excitation wavelength is 532 nm. Atomic force microscopy (AFM, D-5A, Micronano) was used to test the morphology and thickness of the MoS<sub>2</sub> film.

## Electrochemical Tests

All electrochemical measurements were tested on a CHI660E electrochemical workstation (CH Instruments). Electrochemical measurements were performed in three electrode system. The counter electrode, reference electrode and working electrode are carbon rod, Ag/AgCl and MoS<sub>2</sub>/GC respectively. The hydrogen production polarization curve adopts linear sweep voltammetry (LSV), the sweep rate is 5 mV/s, the sweep range is – 0.5 to 0 V, and the electrolyte is 0.5 M H<sub>2</sub>SO<sub>4</sub>. None of the LSV curves were iR corrected. Through the Nernst equation, All the electrochemical potentials were converted into Reversible hydrogen electrode (RHE) voltages:  $E(\text{RHE}) = E(\text{Ag/AgCl}) + 0.159 \text{ V}$ . The frequency ranges of electrochemical impedance spectroscopy (EIS) is 1 Hz–100 kHz, and the overpotential is 200 mV. The cyclic voltammetry (CV) and chronoamperometry (i-t) were used to estimate the stability. The electrochemical double layer capacitance ( $C_{dl}$ ) test adopted the CV curve under different scanning rates. The CV test voltage range was 0.1–0.2 V (vs. RHE), scan rate was 20–140 mV/s. The electrochemically active surface area (ECSA) was calculated from the specific current density through the following relationship:

$$A_{ECSA} = \frac{\text{specific capacitance}}{40 \mu\text{F} \cdot \text{cm}^{-2} \text{ per cm}^2_{ECSA}}$$

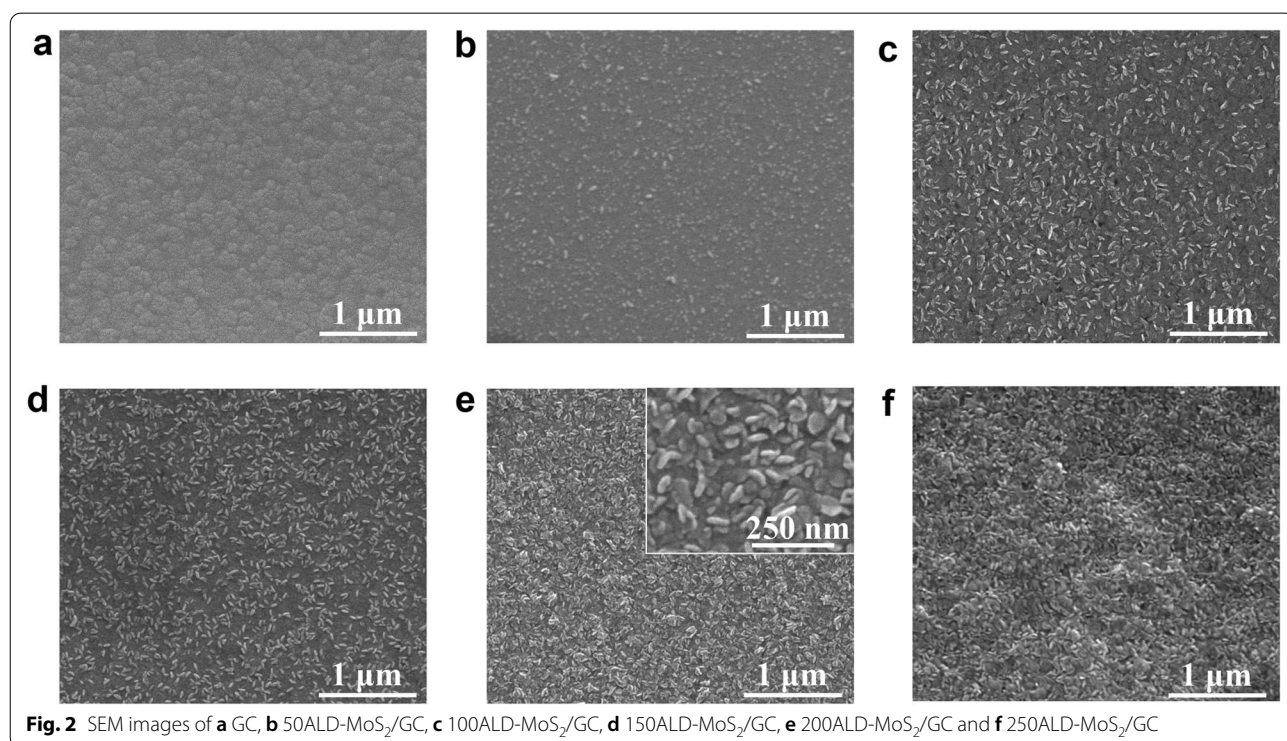
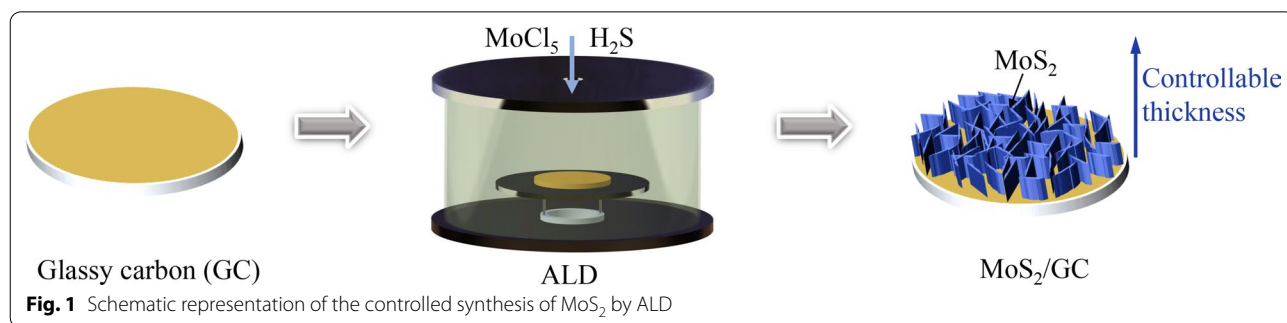
### Results and Discussion

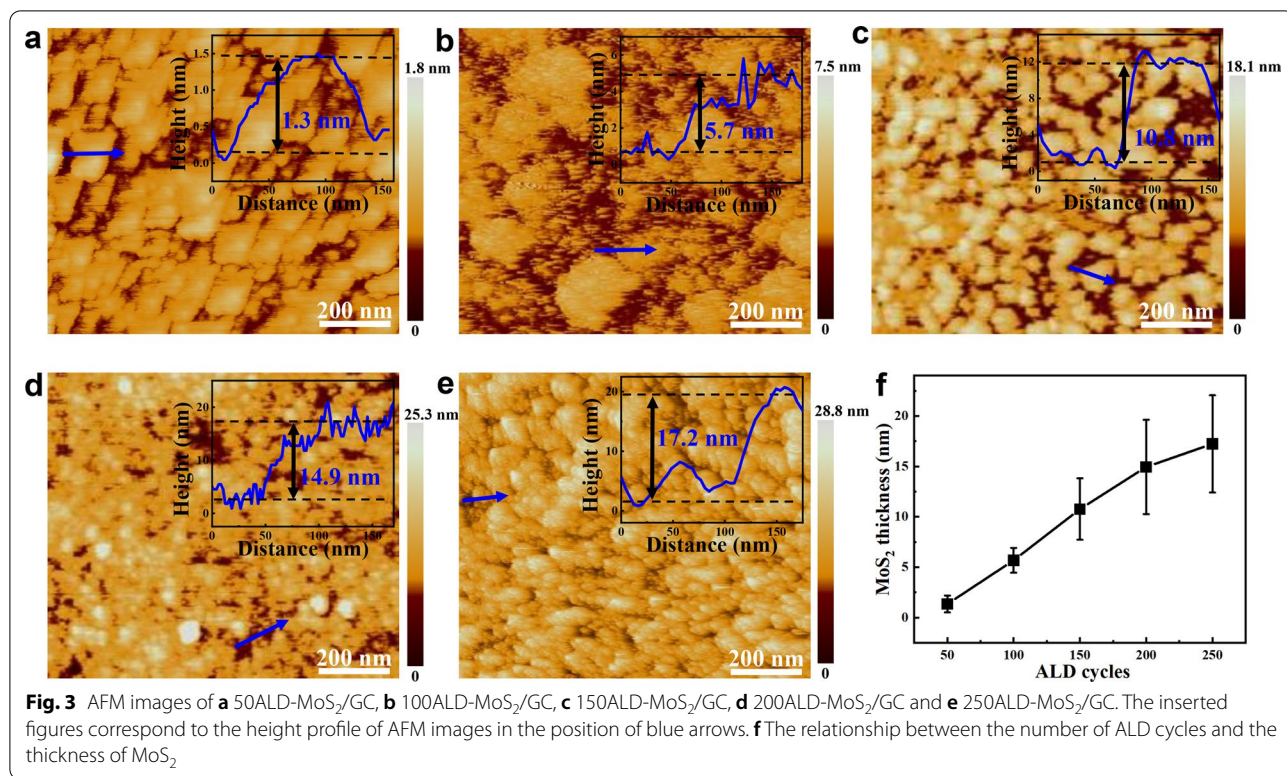
As shown in Fig. 1, MoS<sub>2</sub> films with different thicknesses were prepared on the GC substrate by the ALD with MoCl<sub>5</sub> and H<sub>2</sub>S as precursors under 460 °C. The MoS<sub>2</sub> films prepared at 50, 100, 150, 200 and 250 ALD cycles were named 50ALD-MoS<sub>2</sub>/GC, 100ALD-MoS<sub>2</sub>/GC, 150ALD-MoS<sub>2</sub>/GC, 200ALD-MoS<sub>2</sub>/GC and 250ALD-MoS<sub>2</sub>/GC respectively. MoS<sub>2</sub>/GC can be used directly as a catalytic electrode without the need to load the catalyst on other electrodes through a binder (Nafion), which is

more conducive to the large-scale manufacture and practical application.

From the SEM images (Fig. 2), it can be seen that the MoS<sub>2</sub> films prepared by ALD on the GC substrate has good coverage and consistency. As the number of cycles increases, the MoS<sub>2</sub> films gradually become thicker, and the aggregation states change from nanoparticles to larger nanosheets. When the ALD cycle is low, MoS<sub>2</sub> grows in a direction parallel to the substrate, and when the number of cycles increases, MoS<sub>2</sub> grows vertically to form nanosheets.

The thickness of the MoS<sub>2</sub> on GC is determined by measuring the height profile between the film and the substrate by atomic force microscope (AFM). From the Fig. 3a–e, as the number of ALD cycles increases

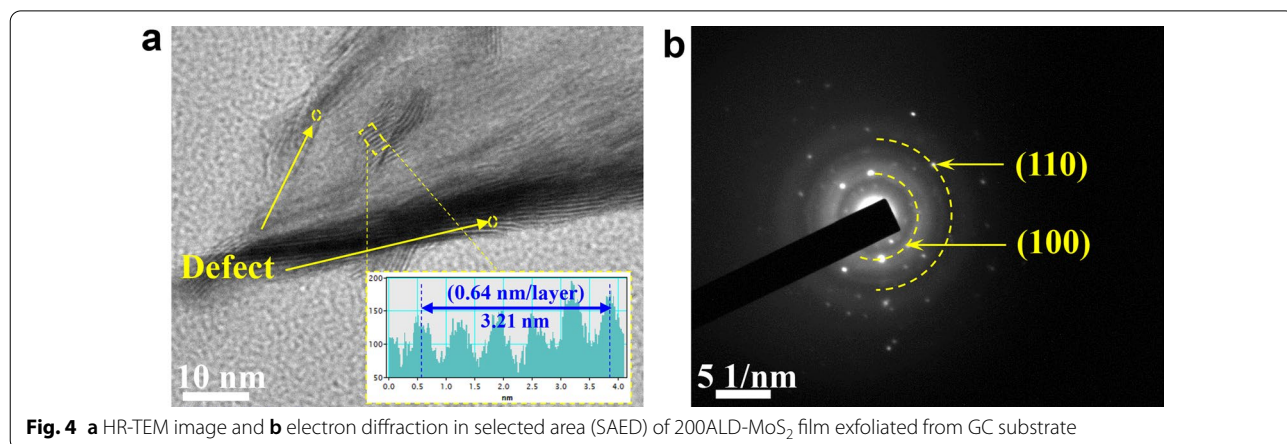




(from 50 to 250), the thickness of the MoS<sub>2</sub> film gradually increases (1.3, 5.7, 10.8, 14.9, and 17.2 nm, respectively). When the number of ALD cycles is 50, the thickness of MoS<sub>2</sub> is about two layers, and the MoS<sub>2</sub> film is not completely continuous. When the ALD cycle number reaches 250, MoS<sub>2</sub> forms dense particles, which causes part of the catalytically active sites to be covered. As shown in Fig. 3f, when the number of cycles increases, the thickness of MoS<sub>2</sub> increases approximately linearly, so that the thickness of MoS<sub>2</sub>

can be precisely controlled. The average manufacturing rate per ALD cycle is approximately 0.69 Å.

Figure 4a is the HR-TEM image of 200ALD-MoS<sub>2</sub>, and the lattice spacing of 0.64 nm corresponds to the (002) crystal plane spacing of MoS<sub>2</sub> [31]. In addition, there are some defects on the MoS<sub>2</sub> nanosheets, which is conducive to HER. In the electron diffraction in selected area (SAED), the inner layer belongs to the (100) crystal plane with 0.26 nm spacing, and the outer layer is the crystal plane with 0.16 nm (110) spacing (Fig. 4b). It can be confirmed that the crystal axis direction is the (001)



direction, which indicates that the sample is composed of multiple layers of 2-D MoS<sub>2</sub> nanoflakes [32].

XRD analysis was performed on the MoS<sub>2</sub> nanosheets, and the results are shown in Fig. 5a. Comparing with the standard card (JCPDS card No. 37-1492), it can be seen that the MoS<sub>2</sub> films has a 2H-phase hexagonal crystal structure. The diffraction peak at 2θ = 14.4° is sharp and strong, which corresponds to (002) lattice plane, indicating that the MoS<sub>2</sub> has a multilayer stack [33]. The diffraction peak at 32.87° corresponding to (100) plane only appears when the number of cycles is greater than 200 cycles, indicating that MoS<sub>2</sub> nanosheets have out-of-plane structure [34]. Except for the carbon peak of the base GC at 16° and 43.7° corresponding to (002) and (100) planes, no other impurity peaks appeared, indicating that there are fewer impurities in the product and the reaction is relatively complete [35].

In the Raman spectrum (Fig. 5b), the vibration peaks of 382 cm<sup>-1</sup> and 404 cm<sup>-1</sup> are caused by the E<sub>2g</sub><sup>1</sup> and A<sub>1g</sub>

vibrational modes of MoS<sub>2</sub>, respectively. The E<sub>2g</sub><sup>1</sup> corresponds to the intramolecular vibration of S atoms relative to Mo atoms. The A<sub>1g</sub> corresponds to only S atoms vibrating in the opposite direction outside the plane [34]. The difference in the peak position distance between the two peaks of MoS<sub>2</sub> is sensitive to the thickness of the MoS<sub>2</sub> film [36]. The position difference between the two peaks of 50ALD-MoS<sub>2</sub>/GC and 100ALD-MoS<sub>2</sub>/GC is 22.3 and 24.1 cm<sup>-1</sup>, respectively. It shows that MoS<sub>2</sub> films are accumulating and thickening in the ALD process, which also proves that the ALD is a precise and controllable preparation method.

A standard three-electrode system was used to evaluate the HER activity of MoS<sub>2</sub> films with different thicknesses in a 0.5 M H<sub>2</sub>SO<sub>4</sub> solution. Before the hydrogen evolution test, the CV test was used to pre-treat the electrode to eliminate some pollutants on the catalyst surface. It can be seen from the polarization curve (Fig. 6a) that the insignificant current density in the curve confirms that

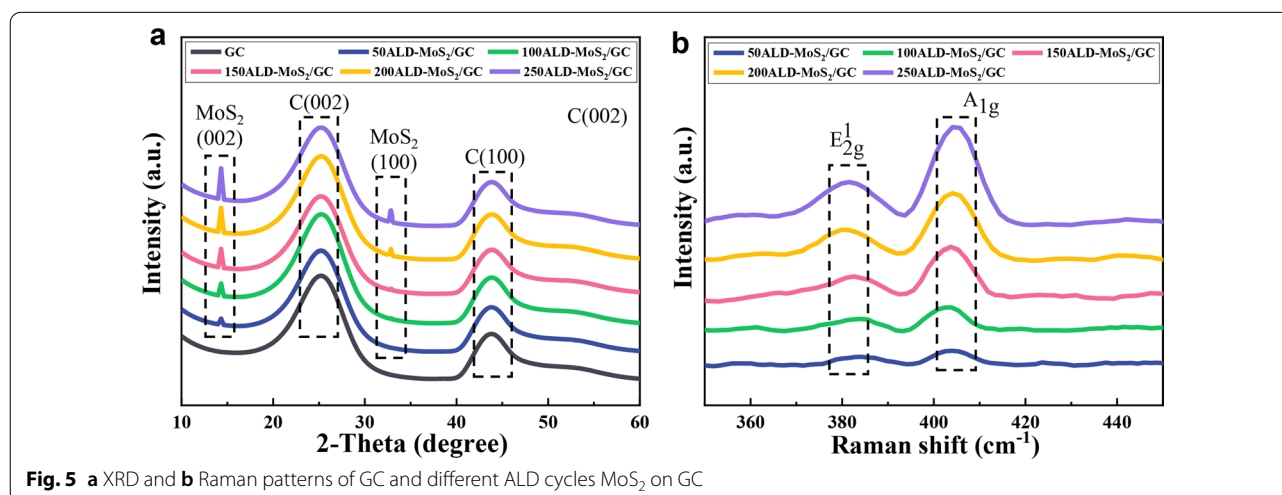


Fig. 5 a XRD and b Raman patterns of GC and different ALD cycles MoS<sub>2</sub> on GC

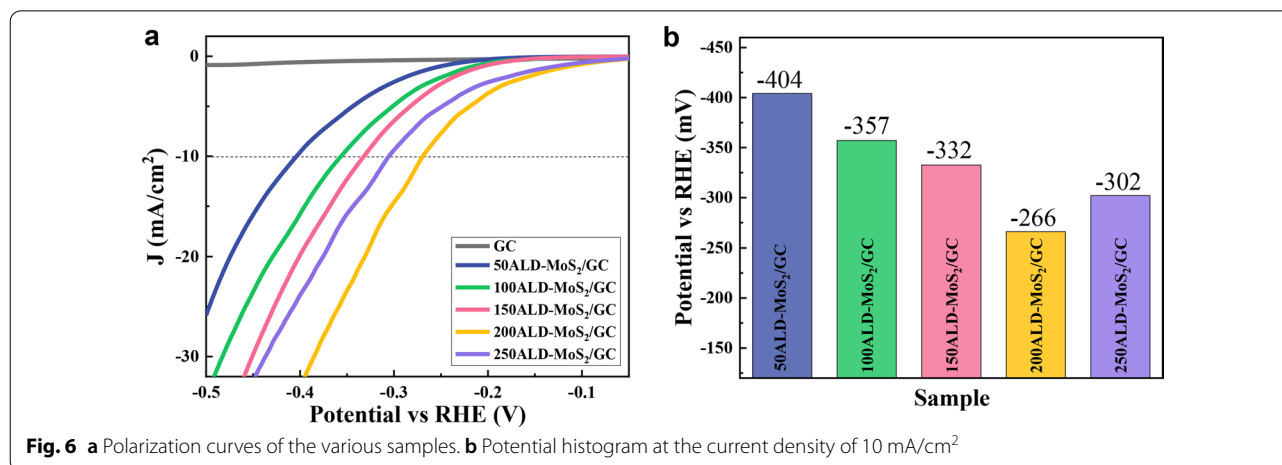


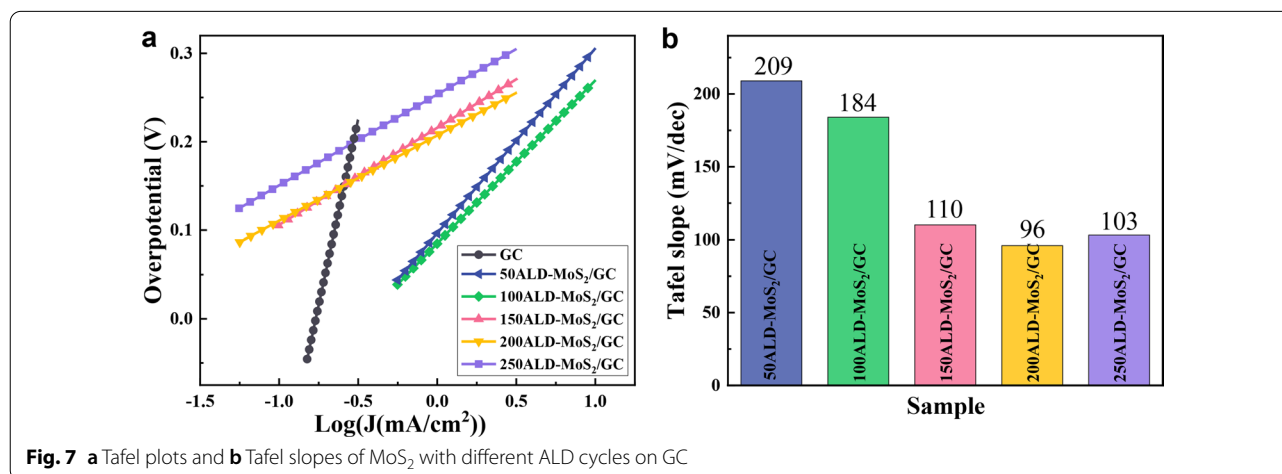
Fig. 6 a Polarization curves of the various samples. b Potential histogram at the current density of 10 mA/cm<sup>2</sup>

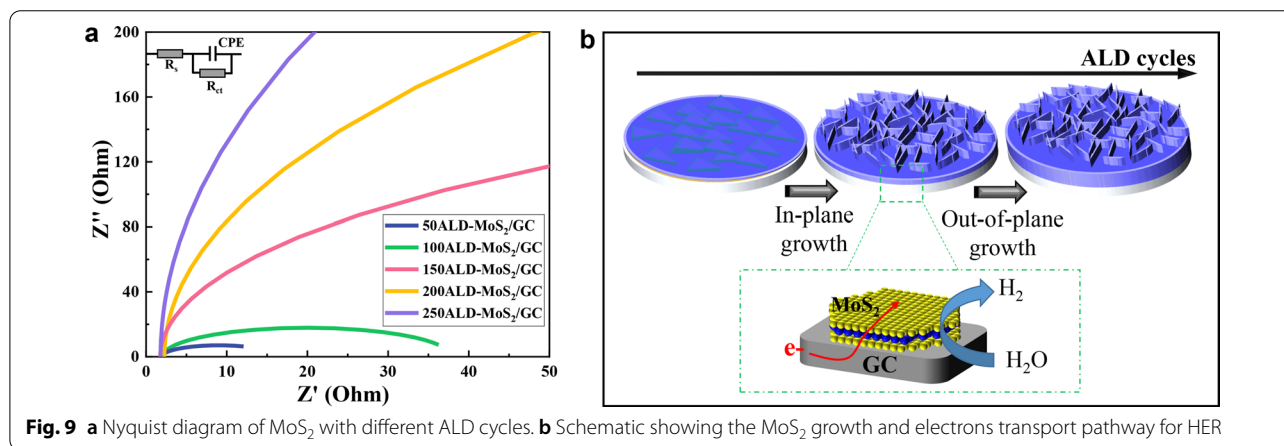
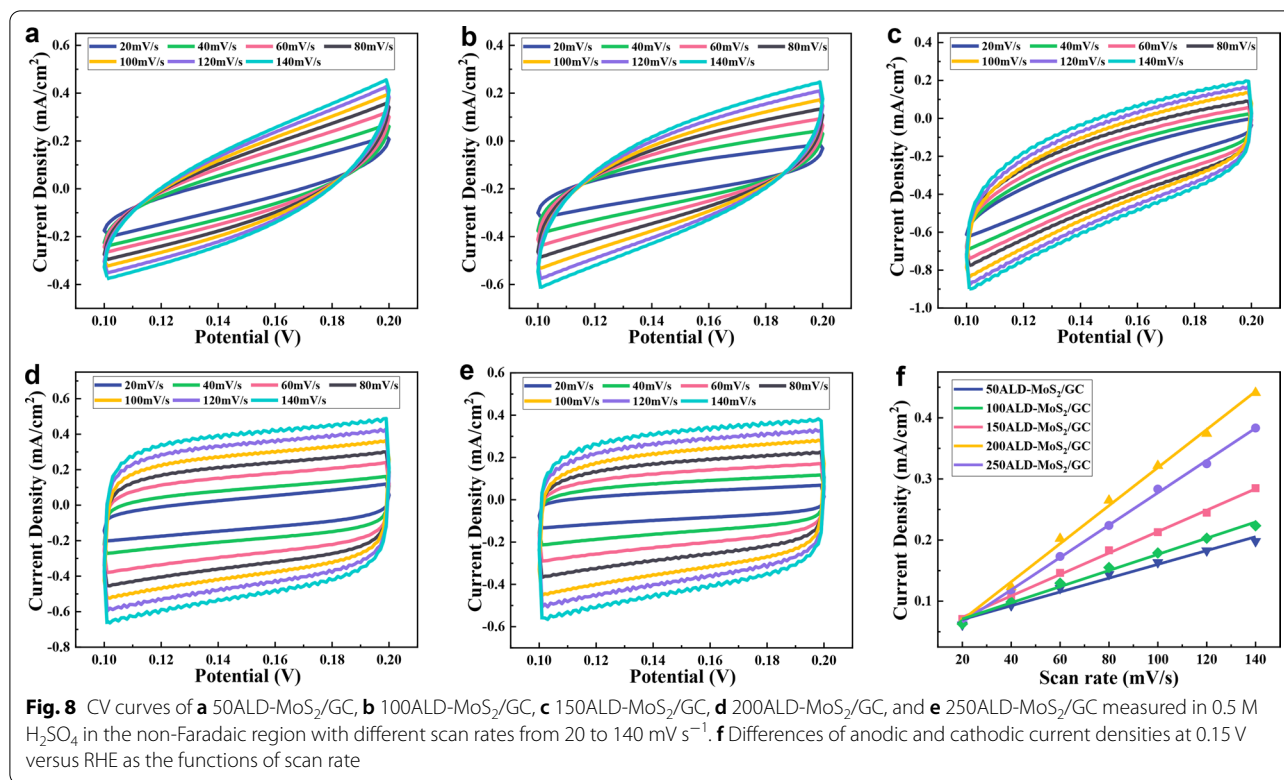
GC has almost no catalytic activity. MoS<sub>2</sub> with different ALD cycles has significantly different catalytic activity, which indicates the effect of MoS<sub>2</sub> with different thicknesses. Figure 6b shows the crossing point when the current density is -10 mA/cm<sup>2</sup>. As the number of ALD cycles is extended from 50 to 200, the HER performance of the MoS<sub>2</sub>/GC gradually improves, because the amount of catalytically active MoS<sub>2</sub> on the GC is increasing. When the number of ALD cycles continued to increase to 250, the catalytic performance decreased, which was due to the poor conductivity of MoS<sub>2</sub> and severe aggregation resulting in a smaller number of active sites exposed. In general, the catalytic active sites on the surface of the catalyst will increase as the cycles increases and tend to be stable. However, an overly thick MoS<sub>2</sub> films can cause the catalyst's conductivity to deteriorate and then increase the overpotential. Therefore, among all the catalysts, 200ALD-MoS<sub>2</sub>/GC shows the best HER activity, with an overpotential of 266 mV when the current density is -10 mA/cm<sup>2</sup>.

Figure 7a, b shows the Tafel curves and Tafel slopes of MoS<sub>2</sub> with different ALD cycles on GC. The Tafel slope of the catalyst is negatively correlated with its electrochemical performance. The order of the Tafel slope of MoS<sub>2</sub> catalysts prepared with different ALD cycles is: 209 mV/dec (50ALD-MoS<sub>2</sub>/GC) > 184 mV/dec (100ALD-MoS<sub>2</sub>/GC) > 110 mV/dec (150ALD-MoS<sub>2</sub>/GC) > 103 mV/dec (250ALD-MoS<sub>2</sub>/GC) > 96 mV/dec (200ALD-MoS<sub>2</sub>/GC). The 200ALD-MoS<sub>2</sub>/GC catalyst has the highest hydrogen evolution performance, and its electron transfer rate is also the fastest. The results also confirmed that the MoS<sub>2</sub>/GC HER rate control step is the Volmer reaction, that is, the generation process of adsorbed hydrogen atoms [37]. When the number of ALD cycles is 200, the amount of hydrogen adsorbed on the catalyst surface is obviously increased, which is beneficial to HER.

The effective electrochemical active area is very important to the HER performance of the catalyst, and it is proportional to the electrochemical double capacitance (C<sub>dl</sub>). The electrochemical active area of the catalysts was compared by measuring the C<sub>dl</sub> by CV, which provided a scientific basis for the performance comparison of the catalysts [38]. Figure 8a–e shows the CV curves of MoS<sub>2</sub>/GC with different thicknesses at different scan rates (20–140 mV/s). The test voltage range of CV is 0.1–0.2 V (this voltage range does not produce Faraday induced current). Subsequently, the 1/2 value of the current density difference at the intermediate potential and the scan rate are used to make a linear fitting curve diagram, and the electrochemical double-layer capacitance value of the material can be estimated from the slope of the curve. Figure 8f shows the linear relationship between current density and scan rate of MoS<sub>2</sub>/GC. The C<sub>dl</sub> of 50ALD-MoS<sub>2</sub>/GC, 100ALD-MoS<sub>2</sub>/GC, 150ALD-MoS<sub>2</sub>/GC, 200ALD-MoS<sub>2</sub>/GC, and 250ALD-MoS<sub>2</sub>/GC are 1.13, 1.32, 1.75, 3.11, and 2.65 mF/cm<sup>2</sup>, respectively. Generally speaking, the active area of MoS<sub>2</sub> increases with the increase of the thickness of MoS<sub>2</sub>, but the ECSA of 250ALD-MoS<sub>2</sub>/GC is lower than that of 200ALD-MoS<sub>2</sub>/GC, indicating that excessive MoS<sub>2</sub> nanosheets would aggregate with each other to form blocks and reduce active sites.

In order to deeply explore the influence of the number of ALD cycles on the HER activity, the electrochemical AC impedance method was used to conduct electrode kinetic tests on different samples, as shown in Fig. 9a. The charge transfer resistance is positively correlated with the thickness of MoS<sub>2</sub>, because MoS<sub>2</sub> has poor conductivity. The influence of MoS<sub>2</sub> thickness on HER performance was further analyzed from the ALD growth process (Fig. 9b). When the thickness of MoS<sub>2</sub> is less than 3 layers, MoS<sub>2</sub> grows in the vertical direction, and the





triangular edge of MoS<sub>2</sub> is the main catalytic site. When the thickness of MoS<sub>2</sub> is greater than 3 layers, MoS<sub>2</sub> growth will change from in-plane to out-of-plane, forming nanosheet-like MoS<sub>2</sub>. Due to the large specific surface area and many active sites of the nanosheets, it is beneficial to improve the catalytic performance. But when the thickness of MoS<sub>2</sub> exceeds 15 nm, the excessive resistance will reduce the electron transfer rate, which deteriorates the electrochemical performance of the catalyst.

Durability and stability are also important indicators for investigating the performance of electrocatalysts [39].

In 0.5 M H<sub>2</sub>SO<sub>4</sub> electrolyte, 200ALD-MoS<sub>2</sub>/GC was continuously scanned by CV, and LSV was performed after 1000 cycles. It can be seen from Fig. 10a that when the current density is -10 mA/cm<sup>2</sup>, the overpotential required before 1000 cycles of the catalyst is approximately 0.26 V, and the overpotential after 1000 turns is about 0.28. In addition, the activity of HER is slightly attenuated, which may be caused by a small amount of catalyst falling off the surface of the electrode. In order to further study the durability of the MoS<sub>2</sub>/GC catalyst, the i-t curve of the catalyst at a current density of -10 mA/cm<sup>2</sup> for 32 h was

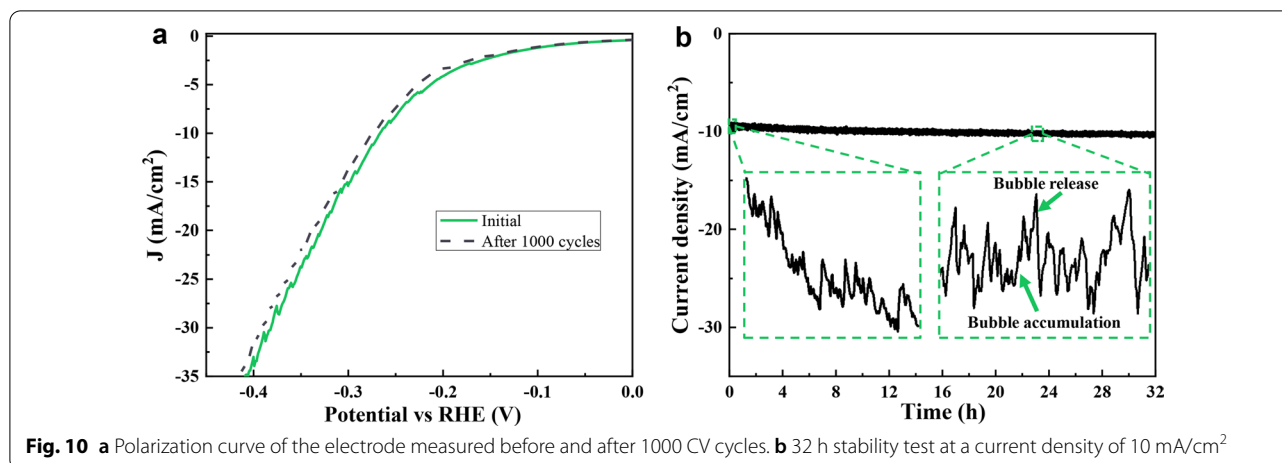


**Table 1** The comparison of MoS<sub>2</sub>-based material for electrochemical hydrogen evolution

Catalysts	Morphology	Electrolyte	$\eta_{10}$ (mV)	Reference
MoS <sub>2</sub>	Monolayer	0.5 M H <sub>2</sub> SO <sub>4</sub>	625	[42]
1 T-2H MoS <sub>2</sub>	Nanosheets	1 M KOH	290	[43]
MCM@MoS <sub>2</sub> -Ni	Nanosheets	0.5 M H <sub>2</sub> SO <sub>4</sub>	263	[44]
MoS <sub>2</sub>	Monolayer	0.5 M H <sub>2</sub> SO <sub>4</sub>	362	[45]
MoS <sub>2</sub> -CN/G	Nanosheets	0.5 M H <sub>2</sub> SO <sub>4</sub>	332	[46]
P-MoS <sub>2</sub>	Nanosheets	0.5 M H <sub>2</sub> SO <sub>4</sub>	250	[47]
1 T-MoS <sub>2</sub>	Layered structure	0.5 M H <sub>2</sub> SO <sub>4</sub>	340	[48]
MoS <sub>2</sub>	Nanosheets	0.5 M H <sub>2</sub> SO <sub>4</sub>	266	This work

investigated. As can be seen from Fig. 10b, the potential of 200ALD-MoS<sub>2</sub>/GC decreased rapidly in the early stage of reaction, which was mainly because the bubbles formed by the adsorption of H<sup>+</sup> in the electrolyte on the electrode surface were not desorbed in time at the early stage of reaction, so a larger overpotential was needed to maintain a fixed current density. With the extension of the reaction time, the attenuation of the curve gradually becomes flat, which is mainly caused by the close agreement between the formation rate of H<sub>2</sub> bubbles on the electrode surface and the desorption rate [40]. Minor fluctuations in the *i*-*t* curve can be attributed to the generation, accumulation and release of hydrogen on the electrode surface during the reaction [41]. The results show that the MoS<sub>2</sub> film manufactured by the ALD method is tightly bonded to the substrate, and has good stability during the HER. As a comparison, other studies about the electrochemical hydrogen evolution performance of MoS<sub>2</sub>-based nanomaterials are summarized in Table 1. It can be seen that the MoS<sub>2</sub> prepared by ALD in this work has better HER performance than many MoS<sub>2</sub>-based composite materials, indicating that

MoS<sub>2</sub> with a suitable thickness can be used as an effective HER catalyst.

### Conclusions

In summary, MoS<sub>2</sub> films with different thicknesses were directly and accurately deposited on the GC substrate by controlling the number of cycles in the ALD process. 200ALD-MoS<sub>2</sub>/GC with 14.9 nm thickness shows the best HER performance, and its overpotential and Tafel slope are - 266 mV and 96 mV/dec<sup>-1</sup>, respectively. The catalytic activity of MoS<sub>2</sub> first becomes better and then deteriorates with the increase of its thickness. Because the dense MoS<sub>2</sub> nanosheets aggregate with each other to reduce the active sites and increase the resistance. In addition, the MoS<sub>2</sub> films prepared by ALD are firmly bonded to the substrate, showing excellent stability. This work reveals that the appropriate thickness of MoS<sub>2</sub> films is beneficial to the optimization of electrocatalytic performance, which has great inspiration for MoS<sub>2</sub> to replace noble metal catalysts for hydrogen evolution.

### Abbreviations

MoS<sub>2</sub>: Molybdenum disulfide; HER: Hydrogen evolution reaction;; GC: Glassy carbon; ALD: Atomic layer deposition; 2-D: Two-dimensional; CVD: Chemical vapor deposition; SEM: Scanning electron microscopy; XRD: X-ray diffraction; HR-TEM: High resolution-transmission electron microscope; SAED: Selected area electron diffraction; LSV: Linear scanning voltammetry; CV: Cyclic voltammetry; EIS: Electrochemical impedance spectroscopy; C<sub>dl</sub>: The double-layer capacitance; RHE: Reversible hydrogen electrode.

### Acknowledgements

Not applicable.

### Authors' contributions

XX: Experiment design, formal analysis, experiment conducting and writing; LL: reviewing and supervision. All authors read and approved the final manuscript.

### Funding

This work is financially supported by the Natural Science Foundation of China (51805248, 62071120).

**Availability of Data and Materials**

All data are fully available without restriction.

**Declarations****Competing interests**

The authors declare that they have no competing interests.

**Author details**

<sup>1</sup>Nanjing Vocational University of Industry Technology, Nanjing 210023, People's Republic of China. <sup>2</sup>School of Mechanical Engineering, Southeast University, Nanjing 211189, People's Republic of China.

Received: 1 May 2021 Accepted: 26 August 2021

Published online: 31 August 2021

**References**

- Zhu J, Hu L, Zhao P et al (2019) Recent advances in electrocatalytic hydrogen evolution using nanoparticles. *Chem Rev* 120(2):851–918
- Jiao Y, Zheng Y, Davey K et al (2016) Activity origin and catalyst design principles for electrocatalytic hydrogen evolution on heteroatom-doped graphene. *Nat Energy* 1(10):1–9
- Eftekhari A (2017) Electrocatalysts for hydrogen evolution reaction. *Int J Hydrogen Energy* 42(16):11053–11077
- Anantharaj S, Kundu S, Noda S et al (2020) Progress in nickel chalcogenide electrocatalyzed hydrogen evolution reaction. *J Mater Chem A* 8(8):4174–4192
- Wang J, Xu F, Jin H et al (2017) Non-noble metal-based carbon composites in hydrogen evolution reaction: fundamentals to applications. *Adv Mater* 29(14):1605838
- Wang H, Gao L et al (2018) Recent developments in electrochemical hydrogen evolution reaction. *Curr Opin Electrochem* 7:7–14
- Cheng N, Stambula S, Wang D et al (2016) Platinum single-atom and cluster catalysis of the hydrogen evolution reaction. *Nat Commun* 7(1):1–9
- Kozejova M, Latyshev V, Kavecansky V et al (2019) Evaluation of hydrogen evolution reaction activity of molybdenum nitride thin films on their nitrogen content. *Electrochim Acta* 315:9–16
- Darband GB, Aliofkhaeaei M, Rouhaghdam AS et al (2019) Three-dimensional Ni-Co alloy hierarchical nanostructure as efficient non-noble-metal electrocatalyst for hydrogen evolution reaction. *Appl Surf Sci* 465:846–862
- Wu J, He J, Li F et al (2017) Ternary transitional metal chalcogenide nanosheet with significantly enhanced electrocatalytic hydrogen-evolution activity. *Catal Lett* 147(1):215–220
- Ling T, Zhang T, Ge B et al (2019) Well-dispersed nickel-and zinc-tailored electronic structure of a transition metal oxide for highly active alkaline hydrogen evolution reaction. *Adv Mater* 31(16):1807771
- Bentley CL, Andronesco C, Smialkowski M et al (2018) Local surface structure and composition control the hydrogen evolution reaction on iron nickel sulfides. *Angew Chem Int Ed* 57(15):4093–4097
- Du H, Kong R, Guo X et al (2018) Recent progress in transition metal phosphides with enhanced electrocatalysis for hydrogen evolution. *Nanoscale* 10(46):21617–21624
- Lau V, Mesch M, Duppel V et al (2015) Low-molecular-weight carbon nitrides for solar hydrogen evolution. *J Am Chem Soc* 137(3):1064–1072
- Laurent C, Scenini F, Monetta T et al (2017) The contribution of hydrogen evolution processes during corrosion of aluminium and aluminium alloys investigated by potentiodynamic polarisation coupled with real-time hydrogen measurement. *Npj Mater Degrad* 1(1):1–7
- Li Y, Yin K, Wang L et al (2018) Engineering MoS<sub>2</sub> nanomesh with holes and lattice defects for highly active hydrogen evolution reaction. *Appl Catal B* 239:537–544
- Zhu J, Wang Z, Dai H et al (2019) Boundary activated hydrogen evolution reaction on monolayer MoS<sub>2</sub>. *Nat Commun* 10(1):1–7
- Dai X, Du K, Li Z et al (2015) Enhanced hydrogen evolution reaction on few-layer MoS<sub>2</sub> nanosheets-coated functionalized carbon nanotubes. *Int J Hydrogen Energy* 40(29):8877–8888
- Wang Z, Li Q, Xu H et al (2018) Controllable etching of MoS<sub>2</sub> basal planes for enhanced hydrogen evolution through the formation of active edge sites. *Nano Energy* 49:634–643
- Rasamani K, Alimohammadi F, Sun Y et al (2017) Interlayer-expanded MoS<sub>2</sub>. *Mater Today* 20(2):83–91
- Chua CK, Loo AH, Pumera M et al (2016) Top-down and bottom-up approaches in engineering 1T phase Molybdenum Disulfide (MoS<sub>2</sub>): towards highly catalytically active materials. *Chem Eur J* 22(40):14336–14341
- Sun J, Li X, Guo W et al (2017) Synthesis methods of two-dimensional MoS<sub>2</sub>: a brief review. *Curr Comput Aided Drug Des* 7(7):198
- Liu H, Wong S, Chi D et al (2015) CVD growth of MoS<sub>2</sub>-based two-dimensional materials. *Chem Vap Deposition* 21:241–259
- Chae W, Cain J, Hanson E et al (2017) Substrate-induced strain and charge doping in CVD-grown monolayer MoS<sub>2</sub>. *Appl Phys Lett* 111(14):143106
- Kim HG, Lee HBR et al (2017) Atomic layer deposition on 2D materials. *Chem Mater* 29(9):3809–3826
- Weber M, Julbe A, Ayril A et al (2018) Atomic layer deposition for membranes: basics, challenges, and opportunities. *Chem Mater* 30(21):7368–7390
- Hao W, Marichy C, Journet C et al (2018) Atomic layer deposition of stable 2D materials. *2D Mater* 6(1):012001
- Tan L, Liu B, Teng J et al (2014) Atomic layer deposition of a MoS<sub>2</sub> film. *Nanoscale* 6(18):10584–10588
- Yue C, Wang Y, Liu H et al (2020) Controlled growth of MoS<sub>2</sub> by atomic layer deposition on patterned gold pads. *J Cryst Growth* 541:125683
- Liu L, Huang Y, Sha J et al (2017) Layer-controlled precise fabrication of ultrathin MoS<sub>2</sub> films by atomic layer deposition. *Nanotechnol* 28(19):195605
- Hu W, Han G, Dai F et al (2016) Effect of pH on the growth of MoS<sub>2</sub> (002) plane and electrocatalytic activity for HER. *Int J Hydrogen Energy* 41(1):294–299
- Wu D, Shi J, Zheng X et al (2019) CVD grown MoS<sub>2</sub> nanoribbons on MoS<sub>2</sub> covered sapphire (0001) without catalysts. *Phys Status Solidi Rapid Res Lett* 13(7):1900063
- Tyagi S, Kumar A, Kumar M et al (2019) Large area vertical aligned MoS<sub>2</sub> layers toward the application of thin film transistor. *Mater Lett* 250:64–67
- Parkin W, Balan A, Liang L et al (2016) Raman shifts in electron-irradiated monolayer MoS<sub>2</sub>. *ACS Nano* 10(4):4134–4142
- Sharma A, Verheijen MA, Wu L et al (2018) Low-temperature plasma-enhanced atomic layer deposition of 2-D MoS<sub>2</sub>: large area, thickness control and tuneable morphology. *Nanoscale* 10(18):8615–8627
- Muehlethaler C, Considine CR, Menon V et al (2016) Ultrahigh Raman enhancement on monolayer MoS<sub>2</sub>. *ACS Photonics* 3(7):1164–1169
- Huang J, Han J, Wu T et al (2019) Boosting hydrogen transfer during Volmer reaction at oxides/metal nanocomposites for efficient alkaline hydrogen evolution. *ACS Energy Lett* 4(12):3002–3010
- Toth PS, Velický M, Slater TJ et al (2017) Hydrogen evolution and capacitance behavior of Au/Pd nanoparticle-decorated graphene heterostructures. *Appl Mater Today* 8:125–131
- Cherevko S, Geiger S, Kasian O et al (2016) Oxygen and hydrogen evolution reactions on Ru, RuO<sub>2</sub>, Ir, and IrO<sub>2</sub> thin film electrodes in acidic and alkaline electrolytes: a comparative study on activity and stability. *Catal Today* 262:170–180
- Zhang Z, Chen Y, Dai Z et al (2019) Promoting hydrogen-evolution activity and stability of perovskite oxides via effectively lattice doping of molybdenum. *Electrochim Acta* 312:128–136
- Huang J, Gao H, Xia Y et al (2018) Enhanced photoelectrochemical performance of defect-rich ReS<sub>2</sub> nanosheets in visible-light assisted hydrogen generation. *Nano Energy* 46:305–313
- Ye G, Gong Y, Lin J et al (2016) Defects Engineered monolayer MoS<sub>2</sub> for improved hydrogen evolution reaction. *Nano Lett* 16(2):1097–1103
- Wang S, Zhang D, Li B et al (2018) Ultrastable in-plane 1T–2H MoS<sub>2</sub> heterostructures for enhanced hydrogen evolution reaction. *Adv Energy Mater* 8:1801345
- Zhang H, Yu L, Chen T et al (2018) Surface modulation of hierarchical MoS<sub>2</sub> nanosheets by Ni single atoms for enhanced electrocatalytic hydrogen evolution. *Adv Funct Mater* 28:1807086
- Kang S, Koo J, Seo H et al (2019) Defect-engineered MoS<sub>2</sub> with extended photoluminescence lifetime for high-performance hydrogen evolution. *J Mater Chem C* 7:10173–10178

46. Yan M, Jiang Q, Yang L et al (2020) Three-dimensional ternary hybrid architectures constructed from graphene, MoS<sub>2</sub>, and graphitic carbon nitride nanosheets as efficient electrocatalysts for hydrogen evolution. *ACS Appl Energy Mater* 3(7):6880–6888
47. Peng C, Song L, Wang L et al (2021) Effect of surface charge distribution of phosphorus-doped MoS<sub>2</sub> on hydrogen evolution reaction. *ACS Appl Energy Mater* 4(5):4887–4896
48. Kim HU, Kim M, Seok H et al (2021) Realization of wafer-scale 1T-MoS<sub>2</sub> film for efficient hydrogen evolution reaction. *Chem Sustain Chem* 14:1344–1350

### Publisher's Note

Springer Nature remains neutral with regard to jurisdictional claims in published maps and institutional affiliations.

**Submit your manuscript to a SpringerOpen<sup>®</sup> journal and benefit from:**

- ▶ Convenient online submission
- ▶ Rigorous peer review
- ▶ Open access: articles freely available online
- ▶ High visibility within the field
- ▶ Retaining the copyright to your article

---

Submit your next manuscript at ▶ [springeropen.com](https://www.springeropen.com)

---